Microchimica Acta (2021) 188: 355
https://doi.org/10.1007/s00604-021-05001-x

ORIGINAL PAPER

Label-free and sensitive MiRNA detection based on turn-on fluorescence of DNA-templated silver nanoclusters coupled with duplex-specific nuclease-assisted signal amplification

Gui-min Ma[1] · Li-wei Huo[1] · Yin-xia Tong[1] · Yu-cong Wang[1] · Cui-ping Li[2] · Hong-xia Jia[1]

Received: 6 April 2021 / Accepted: 24 August 2021 / Published online: 28 September 2021

Abstract

A novel strategy for microRNAs (miRNAs) detection has been developed utilizing duplex-specific nuclease-assisted signal amplification (DSNSA) and guanine-rich DNA-enhanced fluorescence of DNA-templated silver nanoclusters (AgNCs). The combination between target miRNA, DSNSA, and AgNCs is achieved by the unique design of DNA sequences. Target miRNA opens the hairpin structure of the Hairpin DNA probe (HP) by hybridizing with the HP and initiates the duplex-specific nuclease-assisted signal amplification (DSNSA) reaction. The DSNSA reaction generates the release of the guanine-rich DNA sequence, which can turn on the fluorescence of the dark AgNCs by hybridizing with the DNA template of the dark AgNCs. The fluorescence intensity of AgNCs corresponds to the dosage of the target miRNA. This is measured at 630 nm by exciting at 560 nm. The constructed method exhibits a low detection limit (~8.3 fmol), a great dynamic range of more than three orders of magnitude, and excellent selectivity. Moreover, it has a good performance for miR-21 detection in complex biological samples.

Keywords MicroRNAs · DNA template · Silver nanoclusters · Duplex-specific nuclease-assisted signal amplification · Fluorescence enhancement

Introduction

Silver nanoclusters (AgNCs), having sufficiently small size (2~8 Ag atoms), show some molecular-like properties, especially the absorption and emission of light [1]. AgNCs as the emerging fluorophores in recent years have attracted tremendous attention in chemical/biomolecular detection and cellular imaging [2–5]. Compared with other fluorescence materials, AgNCs exhibit smaller size, lower toxicity than quantum dots, and better brightness and photostability than organic dyes. Furthermore, the fluorescence wavelength of the AgNCs depending on the DNA template as a scaffold (DNA-templated AgNCs) is adjustable according to the change of DNA template sequence and its microenvironment. The sensitive response of fluorescence of DNA-templated AgNCs is superior to that of other fluorescence materials, such as quantum dots and organic dyes. This characteristic of DNA-templated AgNCs is beneficial for their application in complex and changeable biological environments [6, 7]. The variations in the microenvironment of the DNA template might give rise to the "turn on" or "turn off" of the fluorescence. Werner et al. have reported that a 500-fold enhancement in red fluorescence of DNA-templated AgNCs is observed in proximity to guanine-rich DNA sequences [8]. It is worth mentioning that using DNA as the template is beneficial to combine with nucleic acid amplification technology to improve the sensitivity of the detection method. And the lower

✉ Hong-xia Jia has been set as the corresponding author. Please check and advise if correct." –>Hong-xia Jia
jhx@hbu.edu.cn

Cui-ping Li
cuipingli@hbu.edu.cn

[1] Key Laboratory of Medicinal Chemistry and Molecular Diagnosis, Ministry of Education; Key Laboratory of Analytical Science and Technology of Hebei Province; Institute of Life Science and Green Development; College of Chemistry and Environmental Science, Hebei University, Baoding 071002, Hebei Province, People's Republic of China

[2] Key Laboratory of Public Health Safety of Hebei Province; Key Laboratory of Medicinal Chemistry and Molecular Diagnosis, Ministry of Education; College of Public Health, Hebei University, Baoding 071002, People's Republic of China

toxicity can increase the compatibility of DNA-templated AgNCs with biological samples. DNA-templated AgNCs have been widely applied in biochemical analysis and detection [9–13].

MicroRNAs (MiRNAs) are single-stranded and non-coding RNA of ~22 nucleotides in length. They can regulate gene expression and contribute to many biological processes. Furthermore, the development of many diseases is also closely associated with the aberrant expression of miRNAs, such as cardiovascular diseases, fibrotic diseases, diabetes, and even cancer [14–18]. Thus, monitoring miRNAs expression levels is crucial for studying miRNA effects and early clinical diagnosis. However, miRNAs exhibit low abundance in vivo and high similarity of homologous sequences. And the series of miRNAs are short. It is not conducive to amplify the signal by polymerase chain reaction (PCR). These unique characteristics make the sensitive detection of miRNAs full of challenges [19]. So, using amplification means is of great significance to improve the sensitivity of miRNA detection.

Conventional approaches for miRNA detection are Northern blotting [20–22] and DNA microarray [23, 24]. They contribute to early miRNA analysis; however, insufficient sensitivity and large sample consumption hamper their application in practice. To overcome the shortcomings, various amplification strategies for miRNA analysis are proposed with improved sensitivity and selectivity, such as real-time polymerase chain reaction (RT-PCR) [25], ligase chain reaction (LCR) [26, 27], rolling circle amplification (RCA) [28–30], exponential amplification reaction (EXPAR) [31], loop-mediated isothermal amplification (LAMP) [32, 33], and duplex-specific nuclease (DSN) signal amplification (DSNSA) [34–36]. Among these amplification approaches, DSN shows a unique advantage owing to its characteristic in the degradation of DNA in DNA-RNA heteroduplex, remaining the RNA intact. The released RNA can be recycled to realize the signal amplification. Furthermore, no polymerase is involved in the DSNSA reaction, which effectively avoided the appearance of non-specific amplification signals caused by polymerases.

MiR-21 plays a crucial role in many biological functions and diseases, such as cardiovascular diseases, inflammation, and cancer. It can regulate various immunological and development processes. MiR-21 has become an attractive target for genetic diagnosis and therapy in many disease conditions [37]. Herein, by integrating the DSNSA as amplification means and guanine-rich DNA-enhanced fluorescence of DNA-templated AgNCs for signal readout, a turn-on fluorescence strategy for miRNA-21(miR-21) detection is developed. The proposed method shows high sensitivity (D.L.~8.3 fmol), excellent selectivity, and good performance for miR-21 detection in complex biological samples.

Experimental section

Materials and apparatus

Silver nitrate ($AgNO_3$) is purchased from Tianjin Fengchuan Chemical Reagent Co., Ltd. (Tianjin, China, http://www.tjhxsj.com/). Sodium borohydride ($NaBH_4$) is obtained from Sigma Aldrich (Shanghai) Trading Co., Ltd. (Shanghai, China, https://www.aladdin-e.com/). Duplex-specific nuclease (DSN) is obtained from Evrogen Joint Stock Company (Moscow, Russia, http://evrogen.com/). 1 mol/L Tris (pH = 8) and 1 mol/L $MgCl_2$ are obtained from ThermoFisher Scientific (China) Co., Ltd. (Shanghai, China, https://www.thermofisher.com/cn/zh/home.html). RNAiso for small RNA kit, Recombinant RNase Inhibitor, the RNase-free water, and DNA and RNA sequences are obtained from TaKaRa Biotechnology Co. Ltd. (Dalian, China, http://www.takara.com.cn/).

The DSNSA reaction is performed on a 2720 Thermal Cycler (Applied Biosystems, Thermo Fisher Scientific Inc. USA, http://www.thermofisher.com/cn/zh/home.html). The fluorescence of AgNCs is recorded by a Fluorolog 3-211 fluorescence spectrophotometer (Horiba Jobin Yvon, France, https://www.horiba.com/cn/). The UV-vis absorption spectra are measured on a TU-1901 double-beam UV-visible spectrophotometer (Beijing Purkinje General Instrument Co., Ltd., China, http://www.pgeneral.com/). The TEM image of AgNCs is recorded by FEI Tecnai G2 F20 field emission transmission electron microscope (ThermoFisher Scientific Inc. USA, https://www.thermofisher.cn/cn/zh/home.html).

The sequences of DNA and RNA are as follows (5′-3′):

SsDNA probe: CCCTTAATCCCCCAGTCTGATAAGCTA

Hairpin structure DNA probe (HP):

TAGCTTATCAGACTGGGCTGGGGTGGGTGGGTGGGGTCAACATCAGTCTGATAAGCTA

MicroRNA-21 (MiR-21): UAGCUUAUCAGACUGAUGUUGA

Let-7a: UGAGGUAGUAGGUUGUAUAGUU

MicroRNA-143 (MiR-143): UGAGAUGAAGCACUGUAGCUC

MicroRNA-221 (MiR-221): AGCUACAUUGUCUGCUGGGUUUC

MicroRNA-396 (MiR-396): UUCCACAGCUUUCUUGAACUG

MicroRNA-172 (MiR-172): AGAAUCUUGAUGAUGCUGCAU

SsDNA probe-a: CCCTTAATCCCCCAGCCTACTACCTCA

HP-a:TGAGGTAGTAGGCTGGGCTGGGGTGGGTGGGTGGGGAACTATACAACCTACTACCTCA

Let-7b: UGAGGUAGUAGGUUGUGUGGUU
Let-7c: UGAGGUAGUAGGUUGUAUGGUU
The experiment buffer solutions are as follows:
10× DSN reaction buffer: 500 mM Tris-HCl, pH 8.0; 50 mM $MgCl_2$
10× PB buffer: 200 mM PB, 0.5 M NaCl, pH 6.6

Preparation of the dark silver nanoclusters

According to the literature method, the dark silver nanoclusters (AgNCs) are prepared via the reduction of $AgNO_3$ by $NaBH_4$ [38]. The detailed preparation of AgNCs is shown in the ESI. The concentration of dark AgNCs is calculated by the concentration of ssDNA probe. 10 μmol/L dark AgNCs are prepared.

Duplex-specific nuclease signal amplification and fluorescence detection

Firstly, 75 pmol HP is heated to 95 °C for 5 min, naturally cooled to room temperature, and then kept for 1 h to form hairpin structures. 75 pmol HP, 4 U Recombinant RNase Inhibitor, a certain amount of miR-21, and 0.2 U DSN are mixed with 1× DSN reaction buffer in the total volume of 10 μL. The mixture is kept for 120 min at 52 °C to perform the DSNSA reaction. Subsequently, 4 μL 10 μmol/L dark AgNCs and 5 μL 10× PB are added into the above reaction solution. After that, 31 μL double distilled water is added to meet the final volume of the mixture of 50 μL. The mixture is incubated for 60 min at 25 °C so that the products of DSNSA can hybridize with the ssDNA probe of dark AgNCs completely. After two-fold dilution of the resulting solution, the fluorescence spectra are recorded from 580 to 720 nm with an excitation wavelength of 560 nm. The fluorescence intensities are determined at 630 nm by exciting at 560 nm. The slit width is 6 nm. All the fluorescence intensities are analyzed three times, and the results are the average values.

Detection of miR-21 in the Hela cell extract

Small RNA samples are extracted from Hela cells by RNAiso for a small RNA kit following the manufacturer's instructions. The content of Hela cell number is 4.7×10^6/mL in the extract solution. The concentration of small RNA extracted from Hela cells is determined by Nanodrop 2000 to be 1.13 μg/μL. 1.13 μg small RNA is added to determine the concentration of miR-21 according to the procedure described in the "Experimental" section. Additionally, 10 and 15 pmol synthetic miR-21 are added to the 1.13 μg small RNA samples to measure the recovery rates of standard addition under the same conditions.

Results and discussion

The strategy of miRNA assay

The principle of AgNCs-based fluorescence assay for miR-21 is illustrated in Fig.1. A special ssDNA probe has been designed, which contains two sequences. One is the DNA template sequence of synthetic dark AgNCs at its 5′ terminal, which is named "a," indicated with gray. Another is called "b" and marked with black at its 3′ terminal, which can hybridize with the "b'" sequence of HP. HP consists of three parts. One is the recognition sequence of miR-21 at its 3′ terminal (c, blue); b' sequence in black hybridizes with part of "c" sequence to form the stem of HP; the third part is a guanine-rich sequence (g, green) in the ring of HP, which can turn on the fluorescence of the dark AgNCs. Firstly, the ssDNA probe is used to synthesize the dark AgNCs, whose fluorescence is off (Fig.1A). In the presence of miR-21, the hairpin of HP is opened by hybridization between miR-21 and the "c" sequence of HP, forming a DNA-RNA double strand. DSN digests DNA in DNA-RNA heteroduplex selectively, remaining RNA intact. So, "c" sequence in the DNA-RNA heteroduplex is degraded by DSN, resulting in the release of miR-21 and the "b'-g" sequence. The released miR-21 recombines with a new HP to initiate a new reaction of DSN digestion. In this manner, duplex-specific nuclease-assisted signal amplification (DSNSA) is realized, and many "b'-g" sequences are released. The released "b'-g" hybridizes with "b" sequence of dark AgNCs, which narrows the distance between the dark AgNCs and the G-rich sequence and stimulates AgNCs to emit strong red fluorescence. At present, the physical mechanism of the enhancement in red fluorescence of DNA-AgNCs has not been understood. Werner thinks it is due to electron transfer from guanine to the nanoclusters. The prepared dark AgNCs with low fluorescence are non-emissive state. They can serve as electron acceptors. Guanines, with the strongest reduction potential in the four nucleotides, as electron donors can reduce dark AgNCs to emit the bright red fluorescence [8, 39]. By contrast, when miR-21 is absent, the double-stranded structure in the stem of HP is degraded by DSN, generating an ssDNA containing "g" and part of "c." The released ssDNA fails to combine with the DNA of AgNCs. So, the fluorescence of dark AgNCs is still off in the control group.

Characterization of DNA-templated AgNCs

The UV-vis absorption spectrum of DNA-emplated AgNCs is shown in Fig.2. It has three absorption peaks. Comparing with which of the control experiments including $AgNO_3$, DNA, and the mixture of $AgNO_3$ and DNA (Fig.2A), obviously, DNA causes the absorption peak at 260 nm; another two broad and weak bands respectively characterized at 402 nm

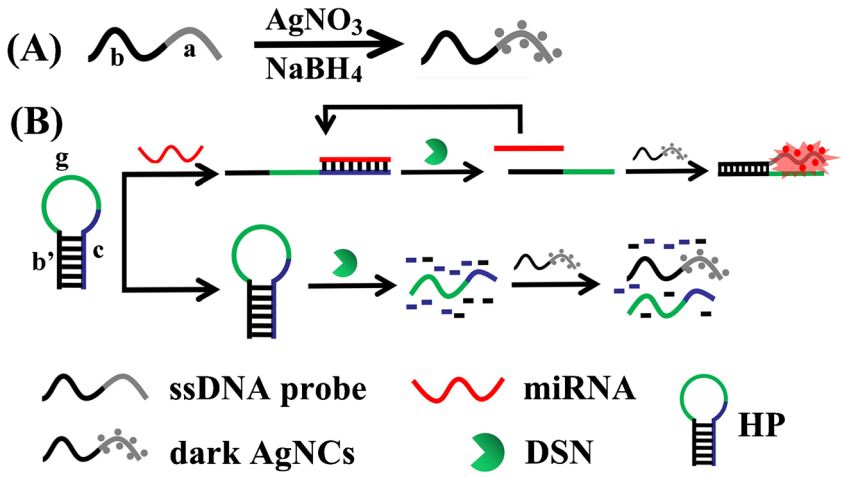

Fig.1 **(A)** Synthesis of dark AgNCs; **(B)** schematic illustration of the miRNA assay based on the turn-on fluorescence of AgNCs coupled with DSNSA

and 445 nm, with no associated fluorescence, may be scattering peaks caused by the aggregation of DNA-AgNCs [40].

Figure 2B shows the excitation and emission spectra of DNA-templated AgNCs. The optimal excitation and emission wavelengths are 560 nm and 630 nm, respectively. Comparing with the fluorescence spectra of control experiments, including the curves of $AgNO_3$, DNA, and the mixture of $AgNO_3$ and DNA (Fig.S1), the fluorescence intensity of AgNCs at 630 nm is stronger than which of the control experiments at the same wavelength. It also proves the formation of fluorescence DNA-templated AgNCs.

From the TEM image of DNA-templated AgNCs (ESI, Fig.S2), we can observe that the AgNCs are spherical. They have varying diameter size. The diameters of the smaller are less than 2 nm, which is in agreement with the value reported for fluorescence AgNCs [1]. However, the diameters of many bigger ones are larger than 2 nm. We think that the bigger may be the aggregation of AgNCs.

Optimization of experimental conditions

In the AgNCs-based homogeneous assay for miR-21, the factors that have the important effect on miR-21 detection have been investigated (see ESI Fig.S3-S7). The optimized dosages of HP, AgNCs, and DSN are 75 pmol, 40 pmol, and 20 U, respectively. The optimized digestion temperature and time for DSN are 52 °C and 120 min.

Fluorescence measurement of miR-21

Under the optimal experimental conditions, the fluorescence signal intensities generated by 0.01~50 pmol of target miR-21 have been measured (Fig.3A). The fluorescence intensity values are linearly dependent on the amount of miR-21 in the ranges of 0.01~0.1 pmol, 0.1~1 pmol, and 1~50 pmol (Fig.3 B, C, and D). The correlation equations are I_f = 1.21 × 10^4 + 2.63 × 10^4 $A_{miR\text{-}21}$(mol) [correlation

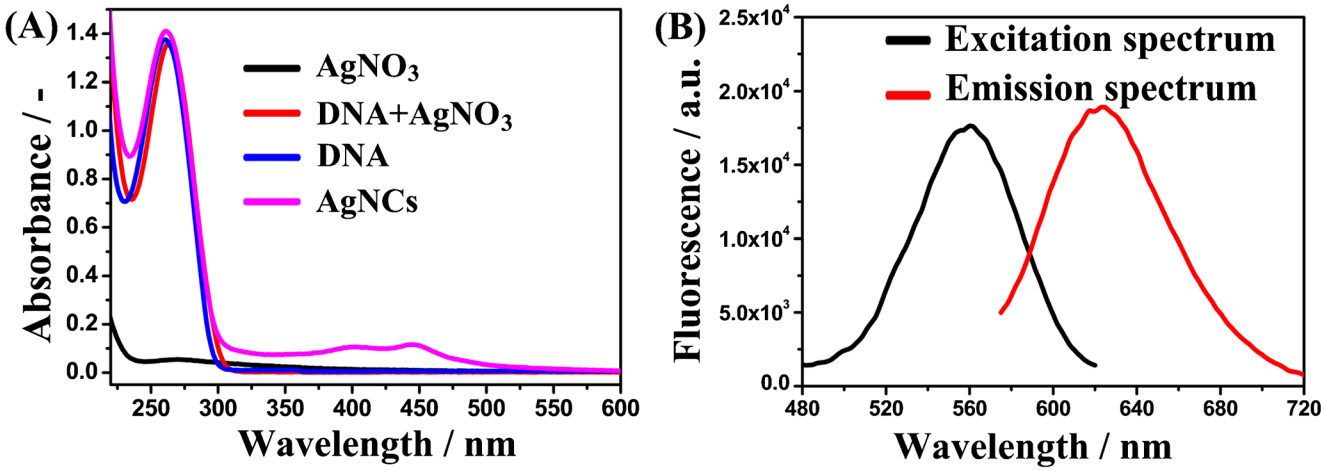

Fig.2 **A** UV-vis absorption spectra of DNA-templated AgNCs (5 μmol/L), $AgNO_3$ (45 μmol/L), DNA (5 μmol/L), and the mixture of DNA (5 μmol/L) and $AgNO_3$ (45 μmol/L). The DNA represents ssDNA probe containing template DNA of AgNCs; **B** excitation and emission spectra of DNA-templated AgNCs. "-" means no unit, and "a.u." means arbitrary unit

Table 1 Comparison of various AgNCs-based fluorescence strategy for miRNA detection

Target miRNA	Amplification	Detection limit	Reference
miRNA-160	None	20 nmol/L	[41]
miRNA-16-5P	SDA[a]	100 nmol/L	[42]
miRNA-141	CHA[b]	297.1 pmol/L	[43]
miRNA-122	SDA	30 pmol/L	[44]
miRNA-21	CHA	38 pmol/L	[45]
miRNA-141	None	1 nmol/L	[46]
miRNA-21	None	10 nmol/L	[46]
miRNA-21	DSNSA	8.3 fmol (83 pmol/L)	Our method

[a] SDA represents the strand displacement amplification

[b] CHA represents the catalytic hairpin assembly reaction

coefficient: $R = 0.9921$], $I_f = 1.37 \times 10^4 + 5.98 \times 10^4$ $A_{miR\text{-}21}$(mol) [$R = 0.9972$], $I_f = 1.89 \times 10^4 + 7.38 \times 10^2$ $A_{miR\text{-}21}$(mol) [$R = 0.9961$], respectively. Thus, the assay has a great dynamic range of more than three orders of magnitude. The proposed method's detection limit is estimated to be 8.3 fmol (3σ, $n = 11$). It is comparable or better than some other AgNCs-based fluorescence methods for miRNA detection. As Table 1 shown, the detection limits of AgNCs-based fluorescence strategies without amplification for miRNA detection is about at the level of nmol/L. It can be improved to pmol/L by adding an amplification technique in the strategy.

The selectivity assay for miR-21 detection

MiR-221, miR-143, let-7a, miR-396, and miR-172 have been selected as a model system to evaluate the selectivity of the proposed miRNA assay. The results are shown in Fig.4. Fluorescence intensities aroused by other miRNAs are all less

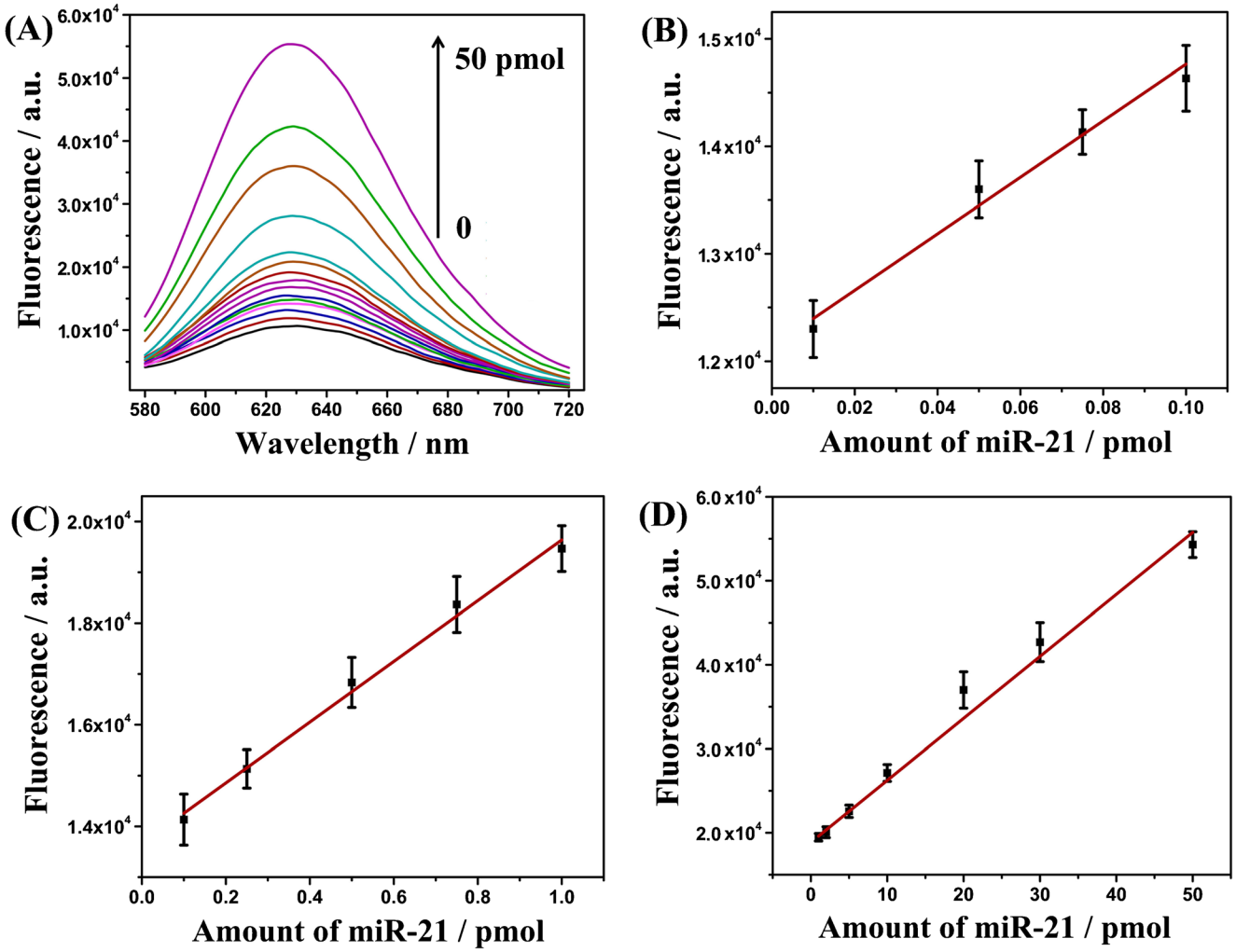

Fig.3 **A** Fluorescence spectra produced by different amounts of miR-21 from 0.01 to 50 pmol. **B**~**D** Relationship between fluorescence intensity and the amount of miR-21 from 0.01 to 0.1 pmol, 0.1 to 1 pmol, and 1 to 50 pmol, respectively. The blank is treated in the same way without miR-21. The fluorescence spectra are measured with excitation wavelengths at 560 nm. The fluorescence intensities are measured at the emission wavelength of 630 nm. Other conditions are performed according to experimental procedures described in the "Experimental" section

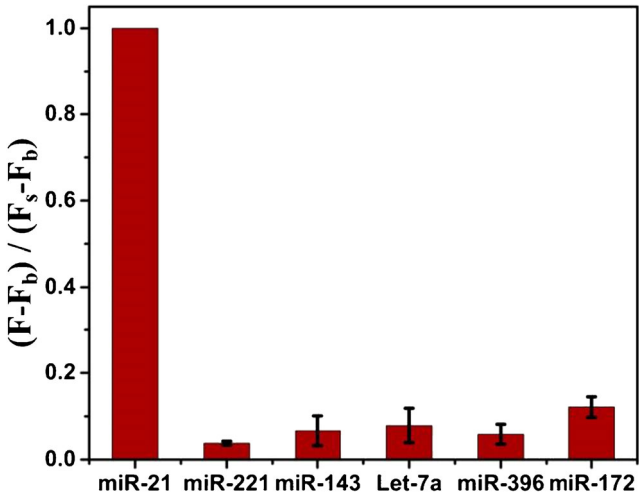

Fig. 4 Selectivity of the proposed assay toward miR-21. The dosage of miRNAs is 30 pmol each. MiR-21 is not added in the determination of interfering miRNAs. The blank is treated in the same way without any miRNAs. F_b represents the fluorescence of blank. F_s represents the fluorescence produced by 30 pmol of miR-21. The fluorescence intensities are measured at the excitation wavelength of 560 nm and the emission wavelength of 630 nm. Other experimental conditions are described in the "Experimental" section

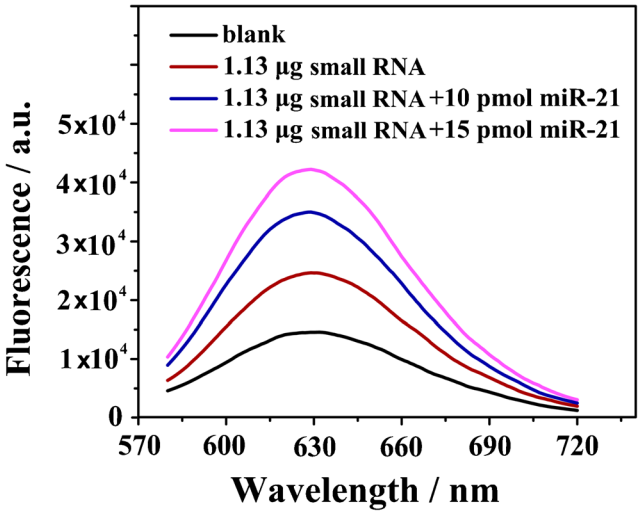

Fig. 5 Detection of miR-21 in the Hela cell extract. The emission spectra are measured with an excitation wavelength of 560 nm. Other experimental conditions are described in the "Experimental" section

than 10% compared with that produced by miR-21 at the same dosage (30 pmol). Therefore, this method has good selectivity for the detection of miR-21.

The selectivity assay for let-7a detection

To further investigate the selectivity of the proposed method in the detection of homologous miRNAs, we take let-7a as the target miRNA and redesign the other DNA probes, ssDNA probe-a, and HP-a. Let-7b and 7c, two homologous sequences most similar to 7a, having only two and one bases different from let-7a, respectively, are selected as the interference. As shown in Fig.S8A, the fluorescence signals aroused by let-7b and 7c are lower than those produced by let-7a. However, they are significantly higher than that triggered by the blank. The fluorescence intensities caused by let-7b and 7c have reached 37% and 56% of that produced by let-7a at the exact dosage (30 pmol) (Fig.S8B). It is a shame that our proposed method has poor selectivity in the detection of homologous miRNA, such as the let-7 family.

Detection of miR-21 in the Hela cell extract

The amount of miR-21 in a small RNA extract solution from Hela cells has been detected with the proposed miRNA assay by the spiked test. The concentration of the small RNA in extract solution has been quantitatively measured by Nanodrop 2000 to be 1.13 μg/μL. As shown in Fig.5, the well-defined signal of miR-21 in the 1.13 μg of small RNA sample has been detected. With the constructed calibration curve (Fig.3D), the amount of miR-21 in the 1.13 μg of small RNA sample is estimated to be 10.16 pmol. The result is verified by adding the synthetic miR-21 (10 and 15 pmol, respectively) to the 1.13 μg of small RNA sample; the spiked recoveries are 110.1% and 108.9%, respectively (Table 2). Therefore, the proposed method can be used to detect miR-21 in the complex biological samples quantitatively.

Conclusions

In this paper, we have developed a label-free and sensitive method for miRNA detection by the combination of fluorescence of DNA-templated AgNCs and DSNSA. Owing to the excellent fluorescence properties of DNA-templated AgNCs and the high amplification efficiency of DSNSA, we have

Table 2 Detection of miR-21 in the Hela cell extract [a]

Sample (μg)	Add (pmol)	Found (pmol)	RSD (n=3) (%)	Recovery (%)
1.13	0	10.16	4.92	–
1.13	10	21.17	4.66	110.1
1.13	20	26.50	3.87	108.9

[a] All the samples were analyzed three times, and the results are the average values

realized the sensitive detection for miR-21 (D.L.~8.3 fmol). And, the synthesis of fluorescence DNA-templated AgNCs is simpler and easier than other fluorescence nanomaterials (see the Table S1). It saves time and cost. The low detection limit, tremendous dynamic range, and excellent selectivity for miR-21 detection provide great potential for practical application in biosensing and clinical assay. However, its poor selectivity in the detection of homologous miRNAs, such as the let-7 family, should not be ignored.

Supplementary Information The online version contains supplementary material available at https://doi.org/10.1007/s00604-021-05001-x.

Funding The project is supported by the National Natural Science Foundation of China (21707027), the Natural Science Foundation of Hebei Province (B2016201052), the Natural Science Foundation of Hebei Education Department (QN2017024), and China Postdoctoral Science Foundation (2017M621094).

Declarations

Conflict of interest The authors declare no competing interests.

References

1. Petty JT, Zheng J, Hud NV, Dickson RM (2004)DNA-templated Ag nanocluster formation. J Am Chem Soc 126:5207–5212. https://doi.org/10.1021/ja031931o
2. Su YT, Lan GY, Chen WY, Chang HT (2010) Detection of copper ions through recovery of the fluorescence of DNA-templatedcopper/silver nanoclusters in the presence of mercaptopropionic acid. Anal Chem 82:8566–8572. https://doi.org/10.1021/ac101659d
3. Guo W, Yuan J, Wang E (2009)Oligonucleotide-stabilized Ag nanoclusters as novel fluorescence probes for the highly selective and sensitive detection of the Hg^{2+} ion. Chem Commun 23:3395–3397. https://doi.org/10.1039/b821518a
4. Shen C, Xia X, Hu S, Yang M, Wang J (2015) Silver nanoclusters-based fluorescence assay of protein kinase activity and inhibition. Anal Chem 87:693–698. https://doi.org/10.1021/ac503492k
5. Han B, Wang E (2011)Oligonucleotide-stabilized fluorescent silver nanoclusters for sensitive detection of biothiols in biological fluids. Biosens Bioelectron 26:2585–2589. https://doi.org/10.1016/j.bios.2010.11.011
6. New SY, Lee ST, Su XD (2016)DNA-templated silver nanoclusters: structural correlation and fluorescence modulation. Nanoscale 8:17729–17746. https://doi.org/10.1039/c6nr05872h
7. Huang Z, Pu F, Lin Y, Ren J, Qu X (2011) Modulating DNA-templated silver nanoclusters for fluorescence turn-on detection of thiol compounds. Chem Commun 47:3487–3489. https://doi.org/10.1039/c0cc05651k
8. Yeh HC, Sharma J, Han JJ, Martinez JS, Werner JH (2010) A DNA-silver nanocluster probe that fluoresces upon hybridization. Nano Lett 10:3106–3110. https://doi.org/10.1021/nl101773c
9. Li J, Zhong X, Zhang H, Le XC, Zhu JJ (2012)Binding-induced fluorescence turn-on assay using aptamer-functionalized silver nanocluster DNA probes. Anal Chem 84:5170–5174. https://doi.org/10.1021/ac3006268
10. Yeh HC, Sharma J, Shih IM, Vu DM, Martinez JS, Werner JH (2012) A fluorescence light-up Ag nanocluster probe that discriminates single-nucleotide variants by emission color. J Am Chem Soc 134:11550–11558. https://doi.org/10.1021/ja3024737
11. Ye T, Chen J, Liu Y, Ji X, Zhou G, He Z (2014) Periodic fluorescent silver clusters assembled by rolling circle amplification and their sensor application. ACS Appl Mater Interfaces 6:16091–16096. https://doi.org/10.1021/am504035a
12. He Y, Jiao B (2017) Determination of the activity of alkaline phosphatase based on the use of ssDNA-templated fluorescent silver nanoclusters and on enzyme-triggered silver reduction. Microchim Acta 184:4167–4173. https://doi.org/10.1007/s00604-017-2459-x
13. He Y, Jiao B (2016) Detection of biotin-streptavidin interactions via terminal protection of small molecule linked DNA and the formation of fluorescent DNA-templated silver nanoclusters. Microchim Acta 183:3183–3189. https://doi.org/10.1007/s00604-016-1968-3
14. Mellis D, Caporali A (2018)MicroRNA-based therapeutics in cardiovascular disease: screening and delivery to the target. Biochem Soc Trans 46:11–21. https://doi.org/10.1042/BST20170037
15. Beermann J, Piccoli MT, Viereck J, Thum T (2016)Non-coding RNAs in development and disease: background, mechanisms, and therapeutic approaches. Physiol Rev 96:1297–1325. https://doi.org/10.1152/physrev.00041.2015
16. Shah P, Bristow MR, Port JD (2017) MicroRNAs in heart failure, cardiac transplantation, and myocardial recovery: biomarkers with therapeutic potential. Current Heart Failure Reports 14:454–464. https://doi.org/10.1007/s11897-017-0362-8
17. Snowhite IV, Allende G, Sosenko J, Pastori RL, Cayetano SM, Pugliese A (2017) Association of serum microRNAs with islet autoimmunity, disease progression and metabolic impairment in relatives at risk of type 1 diabetes. Diabetologia 60:1409–1422. https://doi.org/10.1007/s00125-017-4294-3
18. Lu J, Getz G, Miska EA, Alvarez-Saavedra E, Lamb J, Peck D, Sweet-Cordero A, Ebert BL, Mak RH, Ferrando AA, Downing JR, Jacks T, Horvitz HR, Golub TR (2005) MicroRNA expression profiles classify human cancers. Nature 435:834–838. https://doi.org/10.1038/nature03702
19. Cissell KA, Shrestha S, Deo SK (2007) MicroRNA detection: challenges for the analytical chemist. Anal Chem 79:4754–4761. https://doi.org/10.1021/ac0719305
20. He SL, Green R (2013) Northern blotting. Methods Enzymol 530:75–87. https://doi.org/10.1016/B978-0-12-420037-1.00003-8
21. Várallyay É, Burgyán J, Havelda Z (2008) MicroRNA detection by northern blotting using locked nucleic acid probes. Nat Protoc 3:190–196. https://doi.org/10.1038/nprot.2007.528
22. Calin GA, Dumitru CD, Shimizu M, Bichi R, Zupo S, Noch E, Aldler H, Rattan S, Keating M, Rai K, Rassenti L, Kipps T, Negrini M, Bullrich F, Croce CM (2002) Frequent deletions and down-regulation of microRNA genes miR15 and miR16 at 13q14 in chronic lymphocytic leukemia. Proc Natl Acad Sci 99:15524–15529. https://doi.org/10.1073/pnas.242606799
23. Krichevsky AM, King KS, Donahue CP, Khrapko K, Kosik KS (2003) A microRNA array reveals extensive regulation of microRNAs during brain development. RNA 9: 1274-1281. 10.1261rna.5980303
24. Thomson JM, Parker J, Perou CM, Hammond SM (2004) A custom microarray platform for analysis of microRNA gene expression. Nat Methods 1:47–53. https://doi.org/10.1038/NMETH704
25. Raymond CK, Roberts BS, Garrett-Engele P, Lim LP, Johnson JM (2005) Simple, quantitative primer-extension PCR assay for direct monitoring of microRNAs and short-interfering RNAs. RNA 11:1737–1744. https://doi.org/10.1261/rna.2148705
26. Yan JL, Li ZP, Liu CH, Cheng YQ (2010) Simple and sensitive detection of microRNAs with ligase chain reaction. Chem Commun 46:2432–2434. https://doi.org/10.1039/b923521c
27. Zhang PB, Zhang JY, Wang CL, Liu CH, Wang H, Li ZP (2014) Highly sensitive and specific multiplexed microRNA quantification

using size-coded ligation chain reaction. Anal Chem 86:1076–1082. https://doi.org/10.1021/ac4026384
28. Jonstrup SP, Koch J, Kjems J (2006) A microRNA detection system based on padlock probes and rolling circle amplification. RNA 12:1747–1752. https://doi.org/10.1261/rna.110706
29. Cheng YQ, Zhang X, Li ZP, Jiao XX, Wang YC, Zhang YL (2009) Highly sensitive determination of microRNA using target-primed and branched rolling-circle amplification. Angew Chem Int Ed 48:3268–3272. https://doi.org/10.1002/anie.200805665
30. Zhou C, Huang R, Zhou XM, Xing D (2020) Sensitive and specific microRNA detection by RNA dependent DNA ligation and rolling circle optical signal amplification. Talanta 216:120954. https://doi.org/10.1016/j.talanta.2020.120954
31. Jia HX, Li ZP, Liu CH, Cheng YQ (2010) Ultrasensitive detection of microRNAs by exponential isothermal amplification. Angew Chem Int Ed 49:5498–5501. https://doi.org/10.1002/anie.201001375
32. Li CP, Li ZP, Jia HX, Yan JL (2011)One-step ultrasensitive detection of microRNAs with loop-mediated isothermal amplification (LAMP). Chem Commun 47:2595–2597. https://doi.org/10.1039/c0cc03957h
33. Du WF, Lv MM, Li JJ, Yu RQ, Jiang JH (2016) A ligation-based loop-mediated isothermal amplification (ligation-LAMP) strategy for highly selective microRNA detection. Chem Commun 52:12721–12724. https://doi.org/10.1039/c6cc06160e
34. Yin BC, Liu YQ, Ye BC (2012) One-step, multiplexed fluorescence detection of microRNAs based on duplex-specific nuclease signal amplification. J Am Chem Soc 134:5064–5067. https://doi.org/10.1021/ja300721s
35. Hu ZZ, Chen J, Li WY, Wang Y, Li YX, Sang LJ, Li JM, Zhang QF, Ibupoto ZH, Yu C (2015)Label-free fluorescence turn-on detection of microRNA based on duplex-specific nuclease and a perylene probe. Anal Chim Acta 895:89–94. https://doi.org/10.1016/j.aca.2015.08.028
36. Xu F, Dong H, Cao Y, Lu H, Meng X, Dai W, Zhang X, Al-Ghanim KA, Mahboob S (2016) Ultrasensitive and multiple disease-related microRNA detection based on tetrahedral DNA nanostructures and duplex-specific nuclease-assisted signal amplification. ACS Appl Mater Interfaces 8:33499–33505. https://doi.org/10.1021/acsami.6b12214
37. Kumarswamy R, Volkmann I, Thum T (2011) Regulation and function of miRNA-21 in health and disease. RNA Biol 8:706–713. https://doi.org/10.4161/rna.8.5.16154
38. Vosch T, Antoku Y, Hsiang JC, Richards CI, Gonzalez JI, Dickson RM (2007) Strongly emissive individual DNA-encapsulated Ag nanoclusters as single-molecule fluorophores. Proc Natl Acad Sci 104:12616–12621. https://doi.org/10.1073/pnas.0610677104
39. Heinlein T, Knemeyer JP, Piestert O, Sauer M (2003) Photoinduced electron transfer between fluorescent dyes and guanosine residues in DNA-hairpins. J Phys Chem B 107:7957–7964. https://doi.org/10.1021/jp0348068
40. Maretti L, Billone PS, Liu Y, Scaiano JC (2009) Facile photochemical synthesis and characterization of highly fluorescent silver nanoparticles. J Am Chem Soc 131:13972–13980. https://doi.org/10.1021/ja900201k
41. Yang SW, Vosch T (2011) Rapid detection of microRNA by a silver nanocluster DNA probe. Anal Chem 83:6935–6939. https://doi.org/10.1021/ac201903n
42. Zhang J, Li C, Zhi X, Ramón GA, Liu Y, Zhang C, Pan F, Cui D (2016) Hairpin DNA-templated silver nanoclusters as novel beacons in strand displacement amplification for microRNAs detection. Anal Chem 88:1294–1302. https://doi.org/10.1021/acs.analchem.5b03729
43. Kim H, Kang S, Park KS, Park HG (2018)Enzyme-free and label-free miRNA detection based on target-triggered catalytic hairpin assembly and fluorescence enhancement of DNA-silver nanoclusters. Sensors Actuators B Chem 260:140–145. https://doi.org/10.1016/j.snb.2017.12.137
44. Zhang X, Liu S, Song X, Wang H, Wang J, Wang Y, Huang J, Yu J (2019) DNA three-way junction-actuated strand displacement for miRNA detection using a fluorescence light-up Ag nanocluster probe. Analyst 144:3836–3842. https://doi.org/10.1039/c9an00508k
45. Pan M, Liang M, Sun J, Liu X, Wang F (2018) Lighting up fluorescent silver clusters via target-catalyzed hairpin assembly for amplified biosensing. Langmuir 34:14851–14857. https://doi.org/10.1021/acs.langmuir.8b01576
46. Han Y, Zhang F, Gong H, Cai C (2019) Multifunctional G-quadruplex-based fluorescence probe coupled with DNA-templated AgNCs for simultaneous detection of multiple DNAs and MicroRNAs. Anal Chim Acta 1053:105–113. https://doi.org/10.1016/j.aca.2018.11.062